# Supporting Information

## Frick et al. 10.1073/pnas.1321406111

### SI Materials and Methods

**Cloning.** The gene for human aquaporin 2 (AQP2), codon optimized for production in *Pichia pastoris*, was purchased from GeneArt and amplified by PCR. The primers (Invitrogen) introduced an N-terminal 8xHis-tag followed by a tobacco etch virus (TEV) protease digestion site as well as a stop codon after Pro-242. The amplified sequence was subcloned into the pPICZB vector (Invitrogen) using the *SfuI* and *KpnI* restriction sites. The construct was confirmed by sequencing (MWG Biotech), revealing an unintended introduction of a W2S mutation. The plasmid was linearized and transformed into the AQY1-deficient strain of *P. pastoris* GS115 *aqy1Δ* (1) using electroporation.

**Clone Selection and Protein Overproduction.** An initial clone selection was made by restreaking 40 tranformants on plates containing 2,000 μg/mL of the selection agent Zeocin (2). The protein production in three clones showing the best survival was further investigated in a small-scale (25 mL) production screen. The total membrane fraction from these cells were extracted and analyzed by SDS/PAGE and Western blot using an antibody directed against the His-tag. The clone showing the highest production of AQP2 was chosen for scale-up of production in a 3 L fermentor, typically resulting in 500 g wt cells/L culture after 24 h of MeOH induction. Cells were harvested by centrifugation and stored at -20 °C.

**Cell Lysis and Membrane Isolation.** Cells were thawed at room temperature, diluted 1:3 with breaking buffer (50 mM potassium phosphate, pH 7.5, 5% (vol/vol) glycerol, 2 mM EDTA, 1 mM PMSF) and passed twice through a French Press (Thermo Electron Corporation) at 30,000 psi. Cell debris and unbroken cells were spun down at 10,000 × *g* for 2 × 20 min at 4 °C. The resulting membranes were collected at 160,000 × *g* for 90 min at 4 °C. After washing the membranes in urea buffer (4 M urea, 5 mM Tris·HCl pH 9.5, 2 mM EDTA, 2 mM EGTA), they were recentrifuged at 160,000 × *g* for 120 min at 4 °C. The membranes were once again washed (20 mM Tris pH 8, 20 mM NaCl, 10% glycerol, 2 mM EDTA, 1 mM PMSF) to remove traces of urea and centrifuged as before for 1 h. Finally, the membrane pellet was resuspended in 20 mM Tris pH 8, 20 mM NaCl, 10% glycerol, 1 mM PMSF, and stored at -80 °C until further use.

**Membrane Solubilization and Protein Purification.** Approximately 3.5 g of membranes containing AQP2 diluted to 25 mL with buffer A (20 mM Tris pH 8, 300 mM NaCl), supplemented with Complete EDTA-free protease inhibitor (Roche), was solubilized in 2% (wt/vol) n-nonyl-β-D-glucopyranoside (NG) by dropwise addition from a stock solution of 4% (wt/vol) NG in buffer A. After stirring 1 h in an ice bath, unsolubilized material was pelleted at 180,000 × *g* for 30 min at 4 °C. The supernatant was injected on a HisTrap HP 5 mL column (GE Healthcare) at 0.3 mL/min using binding buffer (20 mM Tris pH 8, 300 mM NaCl, 0.4% NG, 10 mM Imidazole). Loosely bound proteins were washed away with 5 CV Wash buffer (binding buffer with 50 mM Imidazole). Finally, AQP2 was eluted with elution buffer (binding buffer with 300 mM Imidazole). Fractions were analyzed using SDS/PAGE.

Pooled AQP2-containing fractions were digested with TEV protease (3) using a 1:2 AQP2:TEV protease ratio. The digestion mixture was supplemented with 0.5 mM tris(2-carboxyethyl) phosphine and left stirring at 4 °C for 15 h. The buffer was exchanged (20 mM Tris pH 8, 300 mM NaCl, 0.4% NG) using a PD-10 column (GE Healtcare). TEV protease and uncleaved material was removed by injecting the sample on a 5 mL HisTrap HP column (GE Healthcare). The AQP2-containing flowthrough was concentrated to 250 μL in a VivaSpin 50 kDa concentration tube (Sartorius Stedim Biotech GmbH), filtered through a 0.2 μm filter, and injected onto a Superdex 200 300/10HK gelfiltration column (GE Healthcare) equilibrated with 20 mM Tris·HCl pH 8, 300 mM NaCl, 0.4% octylglucose–neopentylglycol (OGNPG). Fractions were analyzed, pooled, and concentrated as described above. The resulting protein concentration was measured using NanoDrop (Thermo Scientific) to 7.5 mg/mL, using $\varepsilon = 39{,}700\ M^{-1}\cdot cm^{-1}$ and $M_w = 31.8$ kDa. Finally, the protein was ultracentrifuged at 90,000 × *g* for 20 min at 4 °C.

**Crystallization.** Crystals were obtained by the hanging drop vapor diffusion technique. The reservoir solution typically contained 20–30% (vol/vol) PEG400, 0.1 M Tris pH 8.0, 0.1 M NaCl, and 0.1 M $MgCl_2$. For setting up drops, 4 μL of reservoir solution was mixed with 1 μL 0.1 M $CdCl_2$. The resulting mixture was mixed with 0.5–1 μL protein sample in a 1:1 ratio and left to equilibrate at 4 °C. Rod-shaped crystals appeared within a few days. After transfer to mother liquor, first containing 26% and then 30% (vol/vol) PEG400, crystals were flash frozen in liquid nitrogen and stored for data collection.

**Data Collection and Structural Determination.** Complete data at 100 K from a frozen crystal were collected using a helical script on beamline ID14-4 of the European Synchrotron Radiation Facility (ESRF), Grenoble, France. Image data were processed using MOSFLM (4) and scaled using SCALA of the CCP4 suite (5). Crystals belonged to space group $P4_2$ with one tetramer in the asymmetric unit. The cell dimensions were a = 119.11 Å, b = 119.11Å, c = 90.62 Å, α = β = γ = 90°. Molecular replacement was carried out using the program Phaser (6) from the CCP4 program suite with a homology model of AQP2 based on the structure of human AQP5 (7) [Protein Data Bank (PDB) ID code 3D9S] as the search model.

The model was subjected to iterative rounds of refinement in BUSTER-TNT (8) with manual rebuilding into CNS-generated composite omit maps between each round (9). noncrystallographic symmetry (NCS) restraints between the four monomers in the tetramer were used as well as translation/libration/screw (TLS) refinement. The model consists of four protein chains (A–D) with the following residues—A2–240, B6–238, C6–241, and D2–233—two $Cd^{2+}$ ions, one $Zn^{2+}$ ion, and 59 water molecules. The final R-factor and free R-factor for this model is 20.2% and 22.5%, respectively. The quality of the model was checked using Procheck (10). For statistics on data collection, refinement, and the model, see Table 1.

**Radioactive Calcium Binding Assay on Total Membranes of Oocytes.** Oocytes were isolated and injected with 10 ng AQP2 cRNA in 50 nL water per oocyte or just water and cultured for 3 d as described (11). Total membranes of oocytes were isolated as described (11) and resuspended in calcium washing buffer [CAWABU (60 mM KCl, 0.5 mM $MgCl_2$, 10 mM Imidazole–HCl pH 7.4)]. Next, the membranes were washed twice in CAWABU. The membranes were resuspended in 100 μL CAWABU per 10 oocytes, and 400 μL CAWABU with 12.5 mCi/mL $^{45}Ca^{2+}$ was added and incubated at room temperature for 15 min. The membranes were spun down, washed twice in a large volume of CAWABU, and resuspended in 200 μL CAWABU. Following transfer to counting tubes, 4 mL of scintillation liquid was added and counted in Tri-Carb 299 TR liquid scintillation counter. High water

permeability confirmed expression of AQP2. Each value consists of three independent groups of 10 oocytes each. The experiments were performed trice. The difference between groups was tested by Student $t$ test. A $P$ value $< 0.05$ was considered statistically significant.


1. Fischer G, et al. (2009) Crystal structure of a yeast aquaporin at 1.15 angstrom reveals a novel gating mechanism. *PLoS Biol* 7(6):e1000130.
2. Öberg F, Sjöhamn J, Conner MT, Bill RM, Hedfalk K (2011) Improving recombinant eukaryotic membrane protein yields in Pichia pastoris: The importance of codon optimization and clone selection. *Mol Membr Biol* 28(6):398–411.
3. van den Berg S, Löfdahl PA, Härd T, Berglund H (2006) Improved solubility of TEV protease by directed evolution. *J Biotechnol* 121(3):291–298.
4. Leslie AG, Powell HR (2007) *Evolving Methods for Macromolecular Crystallography* (Springer, Dordrecht, The Netherlands), pp 41–51.
5. Winn MD, et al. (2011) Overview of the CCP4 suite and current developments. *Acta Crystallogr D Biol Crystallogr* 67(Pt 4):235–242.
6. McCoy AJ, et al. (2007) Phaser crystallographic software. *J Appl Cryst* 40(Pt 4):658–674.
7. Horsefield R, et al. (2008) High-resolution x-ray structure of human aquaporin 5. *Proc Natl Acad Sci USA* 105(36):13327–13332.
8. Bricogne G, et al. (2011) *BUSTER Version 2.10.0* (Global Phasing Ltd., Cambridge, UK).
9. Brünger AT, et al. (1998) Crystallography & NMR system: A new software suite for macromolecular structure determination. *Acta Crystallogr D Biol Crystallogr* 54(Pt 5):905–921.
10. Laskowski RA, Macarthur MW, Moss DS, Thornton JM (1993) PROCHECK: A program to check the stereochemical quality of protein structures. *J Appl Cryst* 26(2):283–291.
11. Kamsteeg EJ, Deen PM (2001) Detection of aquaporin-2 in the plasma membranes of oocytes: A novel isolation method with improved yield and purity. *Biochem Biophys Res Commun* 282(3):683–690.


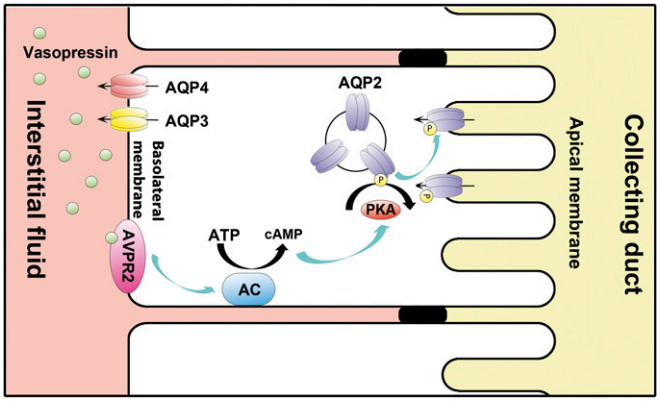


**Fig. S1.** Regulation of AQP2 in the principal cells of the collecting duct. Binding of vasopressin to the vasopressin 2 receptor (AVPR2) in the basolateral membrane leads to increased cAMP formation by adenylate cyclase (AC) and phosphorylation of AQP2 by protein kinase A (PKA) at its C terminus. This phosphorylation event triggers fusion of AQP2-containing storage vesicles with the apical membrane, resulting in increased water permeability. Once water has entered the cell, AQP3 and AQP4 mediate translocation across the basolateral membrane into the interstitial fluid.

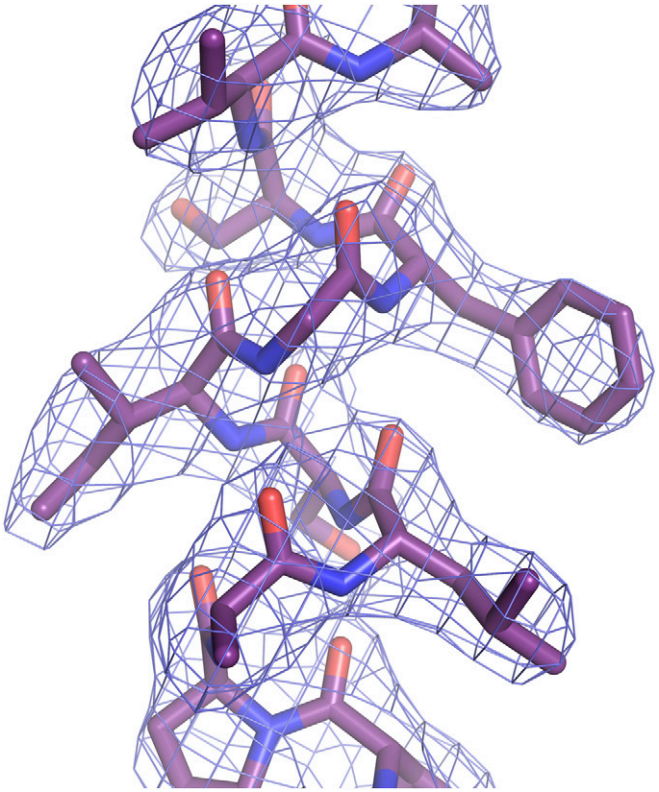

**Fig. S2.** AQP2 electron density. $2F^{obs}$–$F^{calc}$ electron density map around transmembrane (TM) helix 5. Electron density is contoured at 1 σ.

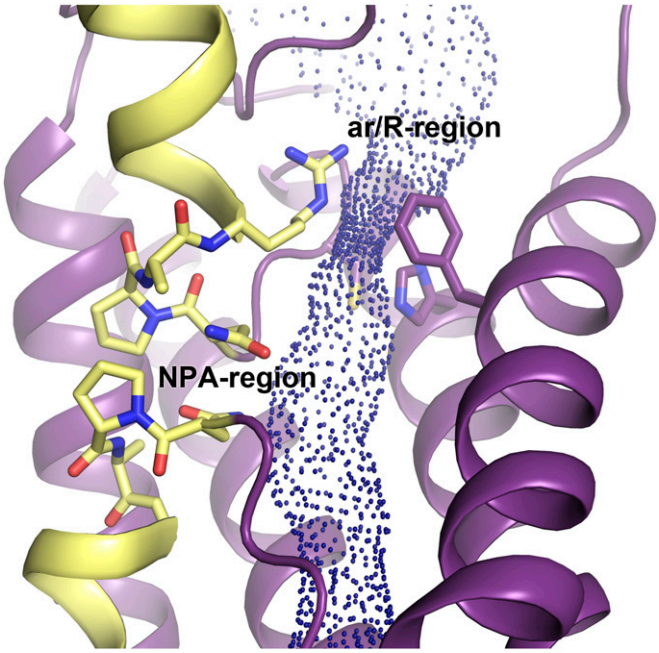


**Fig. S3.** The Asn–Pro–Ala (NPA) region and the selectivity filter [aromatic/arginine (ar/R) region] of AQP2. The half helices in loops B and E are colored yellow. Small blue spheres indicate pore dimensions calculated by HOLE.

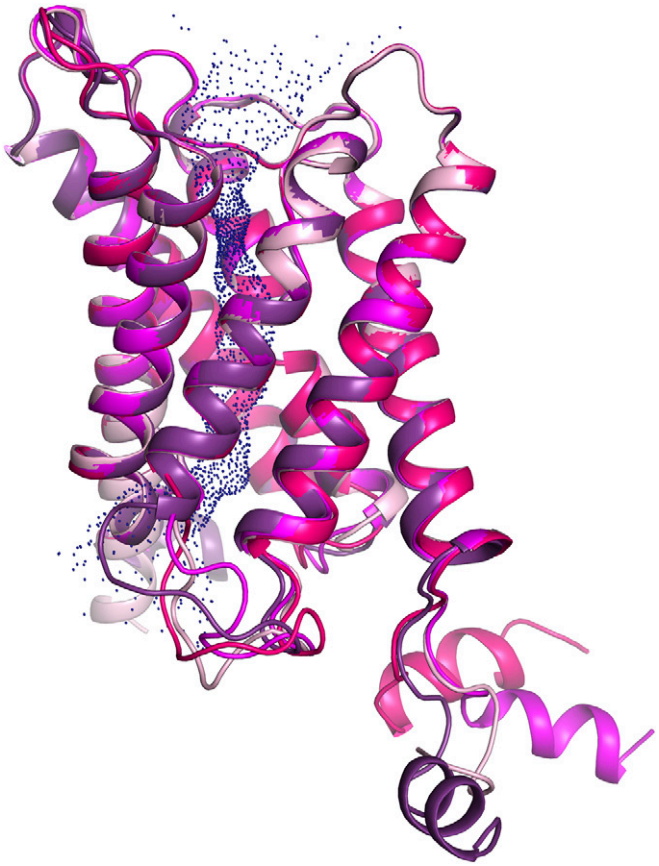

**Fig. S4.** Comparison of AQP2 protomers. Overlay of the four AQP2 protomers showing the flexibility of the C terminus. The blue spheres represent the pore profile, as calculated by HOLE.

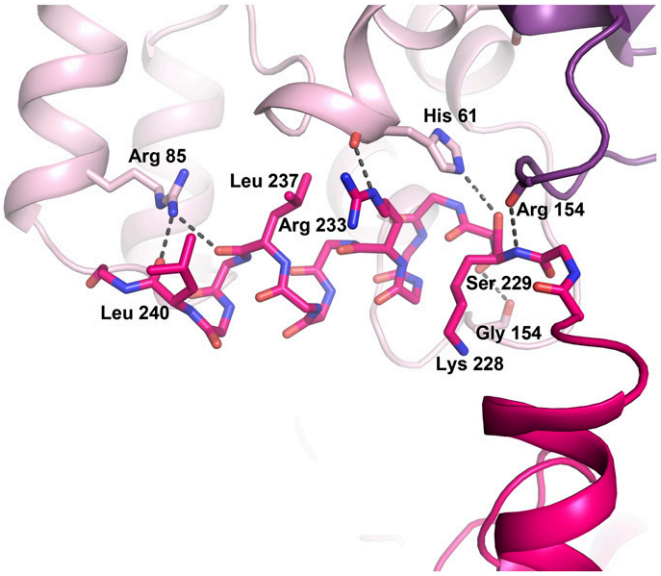


**Fig. S5.** Interactions between C-terminal helix and symmetry-related protomer. The C-terminal helix of protomer C binds into the cytoplasmic vestibule of protomer D. Residues involved in hydrogen bonds (dotted lines) are highlighted.

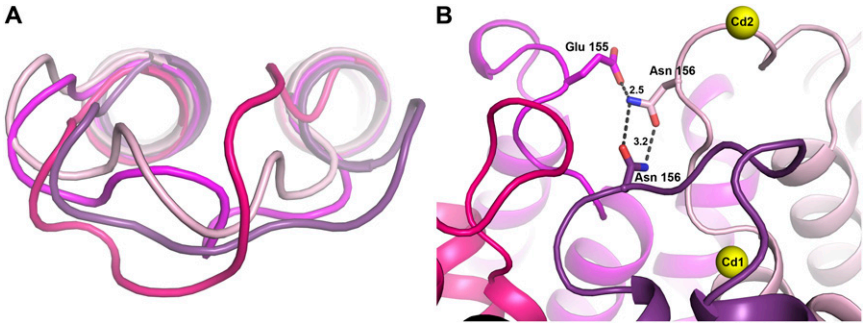


**Fig. S6.** Structure of loop D. (*A*) Overlay of loop D from the four AQP2 protomers showing high conformational variability. (*B*) Interactions between loop D from protomers A, B, and D at the center of the tetramer. Residues involved in hydrogen bonds (dotted lines) are highlighted with distances shown in Å. $Cd^{2+}$ ions are shown as yellow spheres.

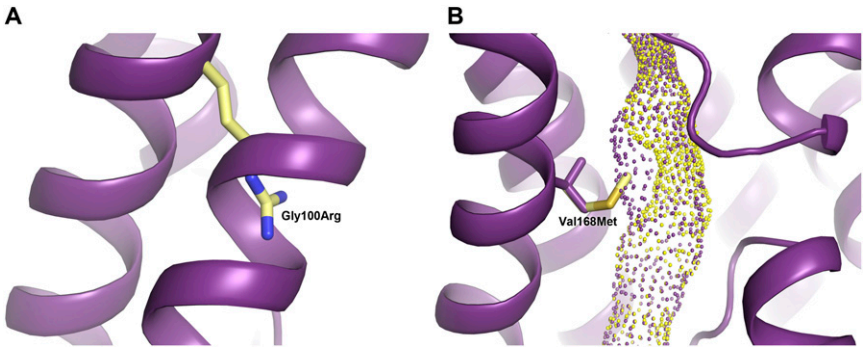


**Fig. S7.** Nephrogenic diabetes insipidus (NDI)-causing mutations in the pore-forming region. (*A*) NDI-causing mutations are often found at helix–helix interfaces, here exemplified by G100R. Gly100 is situated in TM helix 3, and mutation of this residue to arginine (yellow) is likely to disturb its packing against TM helix 1. (*B*) Example of NDI-causing mutation within the water-conducting pore. Mutation of Val168 (purple) to methionine (yellow) causes significant pore narrowing, as indicated by the pore dimensions calculated by the program HOLE (purple and yellow spheres).

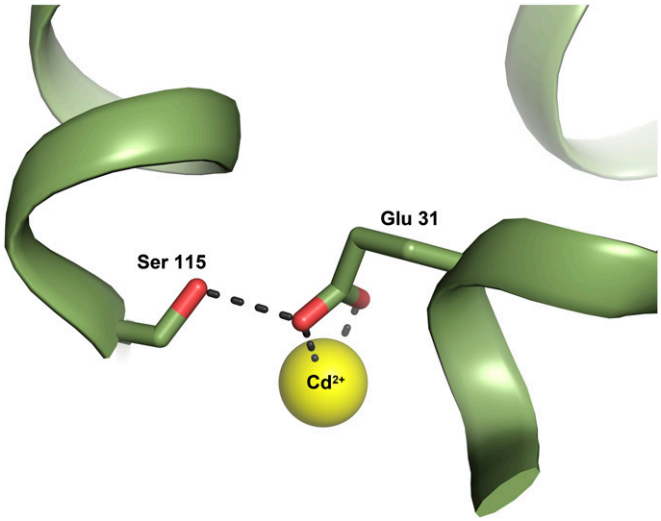


**Fig. S8.** Interactions between the $Cd^{2+}$ binding site and Ser-115 in SoPIP2;1. The spinach water channel plasma membrane intrinsic protein 2;1 (SoPIP2;1) is gated by phosphorylation of Ser115. In the closed structure of SoPIP2;1 (PDB ID code 1Z98), Ser115 hydrogen bonds (dotted lines) to Glu31, one of the ligands for a $Cd^{2+}$ ion (yellow sphere). When Ser115 is phosphorylated, its interaction with the Glu31 is broken, the $Cd^{2+}$ site is perturbed, and the closed conformation of loop D is destabilized. In AQP2, a similar interaction is seen at the Cd1 site where Ser148 hydrogen bonds to the $Cd^{2+}$ ligand Gln57.